

Suppression of the Sonic Heat Transfer Limit in High-Temperature Heat Pipes

Flavio Dobran

Applied Science Department,
New York University,
New York, NY 10003

The design of high-performance heat pipes requires optimization of heat transfer surfaces and liquid and vapor flow channels to suppress the heat transfer operating limits. In the paper an analytical model of the vapor flow in high-temperature heat pipes is presented, showing that the axial heat transport capacity limited by the sonic heat transfer limit depends on the working fluid, vapor flow area, manner of liquid evaporation into the vapor core of the evaporator, and lengths of the evaporator and adiabatic regions. Limited comparisons of the model predictions with data of the sonic heat transfer limits are shown to be very reasonable, giving credibility to the proposed analytical approach to determine the effect of various parameters on the axial heat transport capacity. Large axial heat transfer rates can be achieved with large vapor flow cross-sectional areas, small lengths of evaporator and adiabatic regions or a vapor flow area increase in these regions, and liquid evaporation in the evaporator normal to the main flow.

1 Introduction

Heat pipes are very useful heat transfer devices in terrestrial and space-based systems. The specific application determines the heat pipe's operating temperature, working fluid, and material of construction, whereas the nature of the application determines the heat pipe's detailed design characteristics such as the internal liquid and vapor flow geometry and external shape. The heat pipe application temperatures may range from the liquid helium temperature at a few degrees Kelvin (for maintaining low temperatures of infrared detectors) to a thousand or more degrees as in the cooling of rocket combustion chambers and envisioned space nuclear reactors.

Dobran (1987a) reviewed the heat pipe technology for terrestrial and space systems applications and found that most of the current heat pipe research and development efforts pertain to the applications to space-based systems (Vanlandingham, 1986; Barthelemy et al., 1986; Desanctis et al., 1986; Sadunas and Lehtinen, 1985). High-temperature heat pipes are envisioned to be used in the space nuclear reactor of about 300 kW_e (Vanlandingham, 1986) with a very compact design and its core operating at about 1000°C (Merrigan et al., 1984; Merrigan, 1986). Because of this requirement, Merrigan et al. (1983) discuss the typical heat transfer conditions of a space nuclear reactor as: (1) 100–200 W/cm² radial power density, (2) 10 kW/cm² axial power density, (3) long adiabatic sections to provide separation between the nuclear core and conversion system, and (4) an operation close to the material limits. To cool such a nuclear reactor use can be made of high-temperature heat pipes with the working fluids potassium, sodium, or lithium, since they offer several favorable characteristics (self-regulation and startup, decay heat removal after reactor shutdown, and a high reliability), provided also that many operating limits, such as the sonic heat transfer limit, can be suppressed or eliminated.

The basic heat pipe configuration is illustrated in Fig. 1. It consists of a container such as a pipe whose interior wall is lined with a porous wick structure saturated with a working fluid. Heat transfer in the evaporator region of the heat pipe causes the liquid in the wick to evaporate and flow into the condenser zone where it is condensed. The return of liquid from the condenser to the evaporator occurs due to the

capillary forces in the wick that create a surface tension pressure difference required to overcome the vapor and liquid pressure drops, including that due to gravitation or other externally imposed body forces. For a given geometry pipe and working fluid, the thermohydrodynamic flow aspects in a heat pipe determine its heat transport limits (Dobran, 1987a). The depletion of liquid on the surface of the evaporator produces the *boiling heat transfer limit*, whereas the porous wick structure is endowed with the *capillary heat transfer limit* where an effective liquid supply (pumping) from the condenser to the evaporator ceases. At high axial heat fluxes and in long heat pipes, the countercurrent flow of liquid and vapor produces the *entrainment heat transfer limit* where any further increase in the vapor flow by heat addition, for example, cannot sustain any more increase in the liquid condensate flow. When the design of a heat pipe overcomes the liquid flow limitations, the vapor flow can produce sonic and viscous flow limiting operations. The *sonic or choked flow heat transfer limit* is produced under the control of the inertial forces in the vapor. Heat addition or mass injection in the evaporator accelerates the vapor and can produce choking at the evaporator exit where the Mach number reaches unity, if the downstream condenser temperature is sufficiently low, as may occur during the startup of a heat pipe. Figure 2 illustrates the experimental data of Kemme (1969) taken in a sodium heat pipe with no adiabatic region. Curve A in this figure corresponds to the subsonic flow in the evaporator and condenser, whereas curve B corresponds to the sonic flow condition at the evaporator exit. Curves C and D correspond to the situations of supersonic flow in the condenser region close to the evaporator and vapor flow deceleration through shocks. The mass withdrawal in the condenser has the tendency to produce large nonuniform-

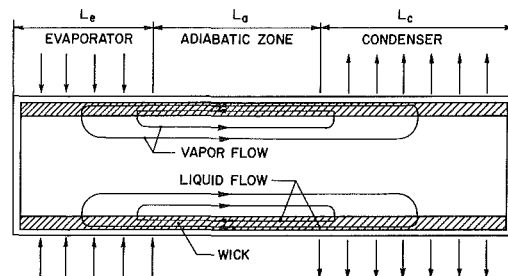


Fig. 1 Basic heat pipe configuration

Contributed by the Heat Transfer Division for publication in the JOURNAL OF HEAT TRANSFER. Manuscript received by the Heat Transfer Division January 5, 1988. Keywords: Heat Pipes and Thermosyphons, High-Temperature Phenomena, Liquid Metals.

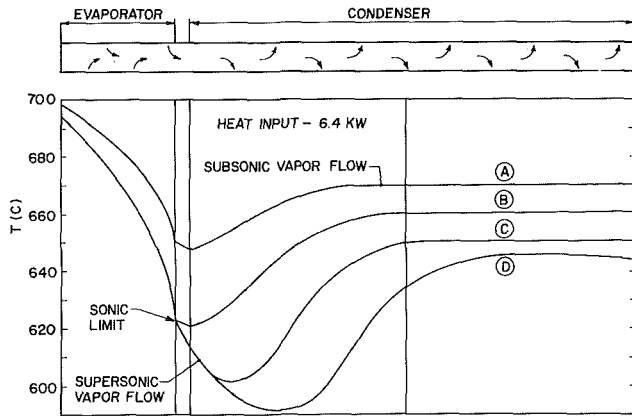


Fig. 2 Temperature distribution in a sodium heat pipe (Kemme, 1969)

ities in flow properties in the radial direction and may yield flow reversals (Busse, 1986). For this reason, the shock regions in the condenser are poorly defined (see Fig. 2). Near the working fluid's freezing point the vapor density is low and a heat pipe is more prone to choking than at higher temperatures. Fluids such as sodium and lithium have low vapor densities and are, therefore, more influenced by the sonic heat transfer limit than other high-vapor-density fluids. A heat pipe operation beyond the sonic heat transfer limit will produce an operation at a higher temperature that may adversely affect the performance of the device transferring the heat to the heat pipe and possibly destroy the heat transfer surfaces. For this reason, a high-temperature heat pipe should not be operated beyond the design temperature and sonic heat transfer limit. When the inertia and viscous forces of vapor are of the same order of magnitude, choking occurs at the condenser inlet, since the subsonic flow in an adiabatic region with friction can only produce a Mach number increase (Shapiro, 1953; Levy and Chou, 1973). With negligible inertia forces, however, choking does not occur (Busse, 1973); the heat transfer increases steadily with decreasing pressure at the evaporator exit and becomes limited by the zero vapor pressure or the *viscous heat transfer limit*.

The objective of this paper is to present an analytical model that may be used to determine the effects of working fluid, vapor flow area, lengths of evaporator and adiabatic regions, and the manner of liquid evaporation into the vapor core of the evaporator on the sonic heat transfer limit in high-

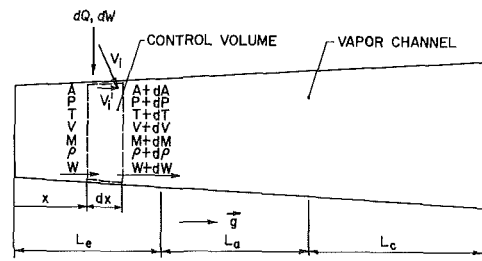


Fig. 3 Definition of the vapor flow variables and control volume for compressible flow analysis

temperature heat pipes. The presented analysis is an extension of previous works (Levy, 1968; Levy and Chou, 1973), which did not systematically and analytically investigate the effects of most of the parameters noted above on the sonic limit heat transfer of high-temperature heat pipes. The methods of suppression of the boiling and wicking heat transfer limits in heat pipes have been discussed by Dobran (1987b).

2 Analysis of the Vapor Flow

The vapor flow thermohydrodynamics in a heat pipe determines the sonic heat transfer limit. For the purpose of determining the first-order effects of vapor flow in a heat pipe, use will be made of one-dimensional, steady-state compressible flow analysis. Figure 3 illustrates the vapor core region and defines the flow variables and a control volume that will be used to derive a set of equations for the analysis. For simplicity, and with a good approximation, the vapor will be assumed to obey a perfect gas equation of state, i.e.

$$P = \rho RT \quad (1)$$

The speed of sound is thus

$$c = (kRT)^{1/2} \quad (2)$$

and the Mach number is defined as

$$M = V/c \quad (3)$$

The conservation of mass and liquid-vapor interface energy balance at an axial position x of the heat pipe give

$$w = \rho VA \quad (4)$$

$$dw = \frac{q}{h_{lv}} dx \quad (5)$$

where dw is positive for the injected mass in the evaporator

Nomenclature

a = factor defined by equation (35)
 A = flow cross-sectional area
 b = factor defined by equation (27)
 c = speed of sound defined by equation (2)
 C = factor defined by equation (34)
 Cp = specific heat at constant pressure
 D = hydraulic diameter
 f = friction coefficient defined by equation (12)
 g = body force per unit mass
 h = enthalpy
 h_{lv} = enthalpy of evaporation
 H = energy term defined by equation (9)
 k = ratio of specific heats

L = heat pipe length
 m = coefficient in equation (18)
 M = Mach number = V/c
 n = coefficient in equation (18)
 P = pressure
 P_{er} = perimeter
 q = heat transfer rate per unit length
 q_s = sonic limit heat transfer rate per unit length
 Q = heat transfer rate
 R = gas constant
 Re = Reynolds number = $wD(1-y_i)/\mu A$
 T = temperature
 V = velocity
 V'_i = axial component of injection velocity, Fig. 3
 w = mass flow rate

x = axial coordinate along the heat pipe
 y_i = V'_i/V
 μ = viscosity
 ρ = density
 τ = shear stress

Subscripts

a = adiabatic region of heat pipe
 c = condenser region of heat pipe
 e = evaporator region of heat pipe
 eff = effective
 i = vapor injection or withdrawal
 l = pertains to the liquid phase
 o = stagnation condition at the evaporator inlet
 s = sonic condition
 v = vapor
 w = wall

and negative for the withdrawn mass in the condenser, and q is the heat transfer rate per unit length of evaporator (positive) or condenser (negative) and represents the heat transfer capability of the working fluid.

Applying the first law of thermodynamics to the control volume in Fig. 3 yields

$$\frac{dQ}{w} = dh + d\left(\frac{V^2}{2}\right) + \left[h - h_i + \frac{1}{2}(V^2 - V_i^2)\right] \frac{dw}{w} \quad (6)$$

where the potential energy terms have been neglected. For an ideal gas, the enthalpy is given as

$$dh = Cp dT \quad (7)$$

so that substituting into equation (6) and using equation (2) we obtain

$$\frac{dQ + dH}{wCpT} = \frac{dT}{T} + \frac{k-1}{2} M^2 \frac{dV^2}{V^2} \quad (8)$$

where

$$dH = -\left(h - h_i + \frac{1}{2}(V^2 - V_i^2)\right) dw \quad (9)$$

represents the effect of injection or nonequilibrium between the liquid-vapor interface and mean vapor core parameters.

The momentum equation gives

$$-AdP - \tau_w P_{er} dx + g\rho A dx = d(wV) - Vy_i dw \quad (10)$$

where

$$y_i = \frac{V_i'}{V} \quad (11)$$

represents the directional effect of the injected or withdrawn mass (see Fig. 3). Using the definition of the friction factor and hydraulic diameter, i.e.

$$f = \frac{\tau_w}{\frac{1}{2}\rho V^2}, \quad D = \frac{4A}{P_{er}} \quad (12)$$

the momentum equation (10) can be written as follows:

$$\frac{dP}{P} + \frac{kM^2}{2} \frac{dV^2}{V^2} + \frac{kM^2}{2} 4f \frac{dx}{D} - M^2 gk \frac{dx}{V^2} + kM^2(1 - y_i) \frac{dw}{w} = 0 \quad (13)$$

where use was made of equations (1) and (3).

From the definition of stagnation temperature, speed of sound, and Mach number we have

$$T_o = T + \frac{V^2}{2Cp} = T\left(1 + \frac{k-1}{2} M^2\right) \quad (14)$$

so that equation (8) can also be written as

$$\frac{dQ + dH}{wCpT} = \left(1 + \frac{k-1}{2} M^2\right) \frac{dT_o}{T_o} \quad (15)$$

Equations (1)-(4) and (13)-(15) give 7 equations with 11 variables $P, \rho, T, c, M, V, T_o, w, A, (dQ + dH)/wCpT$, and

$$4f \frac{dx}{D} - 2g \frac{dx}{V^2} - 2y_i \frac{dw}{w}$$

where four may be chosen as independent. Choosing the last four in this list as independent variables it is then possible to manipulate the above equations and solve for the remaining seven dependent variables. For example, the solutions for the Mach number and pressure distributions are

$$\begin{aligned} \frac{dM^2}{M^2} &= \frac{1 + kM^2}{1 - M^2} \frac{dQ + dH}{wCpT} \\ &+ \frac{kM^2 \left(1 + \frac{k-1}{2} M^2\right)}{1 - M^2} \left[4f \frac{dx}{D} - 2g \frac{dx}{V^2} - 2y_i \frac{dw}{w}\right] \\ &+ \frac{2(1 + kM^2) \left(1 + \frac{k-1}{2} M^2\right)}{1 - M^2} \frac{dw}{w} \\ &- \frac{2 \left(1 + \frac{k-1}{2} M^2\right)}{1 - M^2} \frac{dA}{A} \end{aligned} \quad (16)$$

$$\begin{aligned} \frac{dP}{P} &= -\frac{kM^2}{1 - M^2} \frac{dQ + dH}{wCpT} \\ &- \frac{kM^2(1 + (k-1)M^2)}{2(1 - M^2)} \left[4f \frac{dx}{D} - 2g \frac{dx}{V^2} - 2y_i \frac{dw}{w}\right] \\ &- \frac{2kM^2 \left(1 + \frac{k-1}{2} M^2\right)}{1 - M^2} \frac{dw}{w} + \frac{kM^2}{1 - M^2} \frac{dA}{A} \end{aligned} \quad (17)$$

Equations (16) and (17) are similar to the results of Shapiro (1953), where the influence coefficients multiply the independent variables. In these equations dw can be replaced by the evaporation or condensation heat flux (equation (5)) and the friction coefficient by

$$f = mRe^{-n} \quad (18)$$

$$Re = \frac{\rho(V - V_i')D}{\mu} = \frac{wD(1 - y_i)}{\mu A} \quad (19)$$

where the coefficients m and n depend on whether the flow is laminar or turbulent and with or without the mass injection or withdrawal. For the vapor flow in the adiabatic region of a heat pipe, $y_i = 0$ and m and n may be taken as

$$m = 16, \quad n = 1; \text{ laminar flow (Re} < 2000) \quad (20)$$

$$m = 0.079, \quad n = 0.25; \text{ turbulent flow (Re} \geq 2000)$$

The velocity profile of a laminar incompressible flow in the evaporator has a cosine rather than a parabolic distribution (Busse, 1973; Bankston and Smith, 1971) with

$$m = 2\pi^2, \quad n = 1 \quad (21)$$

In the condenser with high heat transfer rates it is dangerous to use the above analysis and laminar flow expressions for the friction factor owing to the possibility of flow reversals (secondary flow) in this region as discussed previously. High heat fluxes produce high radial Reynolds numbers of the vapor in the evaporator and condenser and yield a turbulent flow in cylindrical condensers even if the axial Reynolds number is below 2000 (Quaile and Levy, 1975).

Equations (16) and (17) can be used to study the effects of the external heat transfer Q , vapor injection and suction y_i , the degree of vapor nonequilibrium $h - h_i$, gravity g , and vapor flow area A , on the limiting heat transfer rates in heat pipes. Thus Levy (1968) neglected the frictional effects, area change, and gravitational effect, and assumed that $dQ + dH = 0$ and $y_i = 0$. From equation (16) it then follows that

$$\frac{dM^2}{M^2} = \frac{2(1 + kM^2) \left(1 + \frac{k-1}{2} M^2\right)}{1 - M^2} \frac{dw}{w} \quad (22)$$

The combination of equation (22) with equation (5) can be integrated from $M(x=0)=0$ and $w(x=0)=0$ to $M(x=L_e)=1$ and $w(x=L_e)=qL_e/h_{lv}$ to obtain an expression for the commonly utilized sonic heat flux limit q_s , i.e.

$$q_s L_e = \frac{\rho_o c_o h_{lv} A}{(2(k+1))^{1/2}} \quad (23)$$

where ρ_o and c_o are the (stagnation) density and speed of sound at the evaporator inlet. When account is also taken of the frictional effects in the above analysis and choking assumed at the condenser inlet, it was found numerically (Levy and Chou, 1973) that the computed heat transfer limits agree better with data than the predictions using equation (23).

To investigate the more general solution of equation (16) we may take $dQ+dH=0$, $g=0$, and assume that the flow is laminar. Thus

(i) Evaporator or Condenser Regions

$$\frac{1-M^2}{M^2(2+(k-1)M^2)} dM^2 = (1+aM^2) \frac{dw}{w} - \frac{dA}{A} \quad (24)$$

where

$$a = k(1-y_i) + \frac{2mk\mu Ah_{lv}}{(1-y_i)D^2 q} \quad (25)$$

(ii) Adiabatic Region

$$\frac{1-M^2}{M^2(2+(k-1)M^2)} dM^2 = bM^2 dx - \frac{dA}{A} \quad (26)$$

where

$$b = \frac{2mk\mu Ah_{lv}}{D^2 q L_e} \quad (27)$$

Moreover, by taking A , y_i , and q constant, the solutions of equations (24) and (26) between any two sections 1 and 2 of the corresponding regions are given by

(i) Evaporator and Condenser Regions

$$\frac{M_2}{M_1} \left[\frac{1 + \frac{k-1}{2} M_1^2}{1 + \frac{k-1}{2} M_2^2} \right]^{1/2} \times \left[\frac{1 + \frac{k-1}{2} M_2^2}{1 + \frac{k-1}{2} M_1^2} \frac{1 + aM_1^2}{1 + aM_2^2} \right]^{\frac{1+a}{1+2a-k}} = \frac{w_2}{w_1} \quad (28)$$

(ii) Adiabatic Region

$$\frac{1}{2} \left[\frac{1}{M_1^2} - \frac{1}{M_2^2} \right] + \ln \left[\frac{M_1^2}{M_2^2} \frac{1 + \frac{k-1}{2} M_2^2}{1 + \frac{k-1}{2} M_1^2} \right]^{(k+1)/4} = b(x_2 - x_1) \quad (29)$$

In particular, the solution represented by equation (23) is a special case of the solution expressed by equation (28). This may be proved by taking in the latter equation $y_i=0$, $\mu=0$ ($a=k$), $w_1=\rho_o c_o M_1 A$, $M_1(x=0)=0$, $M_2(x=L_e)=1$, and $w_2=qL_e/h_{lv}$.

The more useful forms of equations (28) and (29) are obtained by solving these equations for the maximum heat transfer rate q , which occurs when the flow chokes at the exit of the adiabatic region of a heat pipe. Setting in equation (28) $w_1=\rho_o c_o M_1 A$, $M_1(x=0)=0$, $w_2=qL_e/h_{lv}$ and $M_2=M_e$ (exit of evaporator), and in equation (29) $M_1(x=L_e)=M_e$,

$M_2(x=L_e+L_a)=1$ and $x_2-x_1=L_a$, we obtain the following results

$$\frac{qL_e}{h_{lv}\rho_o c_o A} = \frac{M_e}{\left(1 + \frac{k-1}{2} M_e^2\right)^{1/2}} \left[\frac{1 + \frac{k-1}{2} M_e^2}{1 + aM_e^2} \right]^{\frac{1+a}{1+2a-k}} \quad (30)$$

$$\frac{1}{2} \left[\frac{1}{M_e^2} - 1 \right] + \ln \left[\frac{k+1}{2} \frac{M_e^2}{1 + \frac{k-1}{2} M_e^2} \right]^{(k+1)/4} = bL_a \quad (31)$$

and after normalizing by the sonic heat flux limit q_s (equation (23)), it follows that

$$\frac{q}{q_s} = M_e \left[\frac{2(k+1)}{1 + \frac{k-1}{2} M_e^2} \right]^{1/2} \left[\frac{1 + \frac{k-1}{2} M_e^2}{1 + aM_e^2} \right]^{\frac{1+a}{1+2a-k}} \quad (32)$$

$$\frac{1}{2} \left[\frac{1}{M_e^2} - 1 \right] + \ln \left[\frac{k+1}{2} \frac{M_e^2}{1 + \frac{k-1}{2} M_e^2} \right]^{(k+1)/4} = Ck \left(\frac{L_a}{L_e} \right) \left(\frac{q_s}{q} \right) \quad (33)$$

$$C = 2m \left(\frac{\mu}{\rho_o c_o D} \right) \frac{L_e}{D} (2(k+1))^{1/2} \quad (34)$$

$$a = k \left[(1-y_i) + \frac{C}{(1-y_i)} \left(\frac{q_s}{q} \right) \right] \quad (35)$$

In particular, when $L_a=0$ and $M_e=1$ (choking at the evaporator exit), equation (32) is reduced to the form

$$\frac{q}{q_s} = 2 \left[\frac{k+1}{2(1+a)} \right]^{\frac{1+a}{1+2a-k}} \quad (36)$$

Equations (32) and (33) can now be solved for q/q_s in terms of the independent parameters C , k , L_a/L_e , and y_i , or since μ , ρ_o , c_o , and k can be evaluated at the saturation temperature at the evaporator inlet, the independent variables may also be taken as T_{sat} , D , L_a/D , L_a/L_e , and y_i .

3 Discussion of Results

Using equations (32) and (33), Figs. 4 and 5 illustrate the predicted heat transfer rates with the sonic flow at the evaporator and adiabatic section exits, respectively, and a comparison with the sodium, potassium, and cesium data (Kempe, 1966, 1969; Levy and Chou, 1973; Dzakowic et al., 1969). The analytical results in these figures were generated by assuming that $y_i=0$ (normal-to-the-main-flow vapor injection in the evaporator) and using the perfect gas equation of state for the calculation of density and speed of sound at the saturation temperature at the evaporator inlet. As can be seen from these figures, the inclusion of frictional effects into the model produces a superior comparison of analysis with data and reduces the axial heat transport capacities of heat pipes. At high temperatures, some sodium data (Kempe, 1966; Dzakowic et al., 1969) show a deviation from the sonic heat transfer limit behavior and may be associated with the attainment of the wicking heat transfer limit in heat pipes as dis-

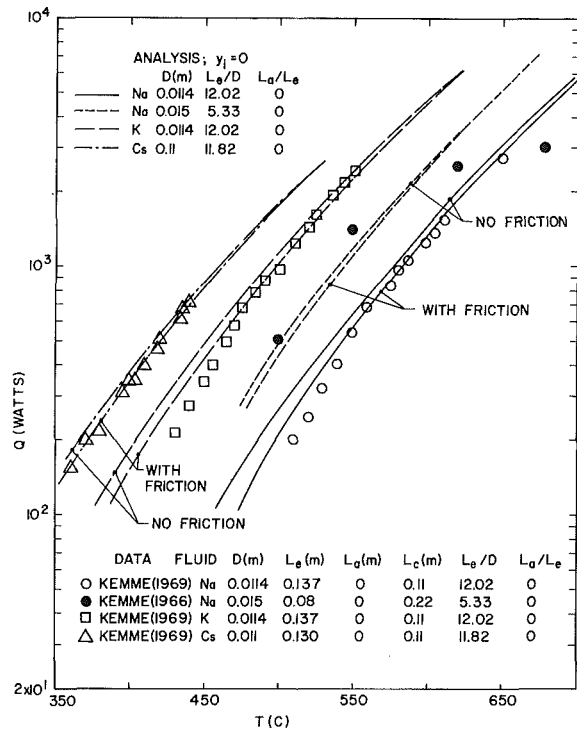


Fig. 4 Comparison of analytic results, with and without friction and choking at the evaporator exit, with data

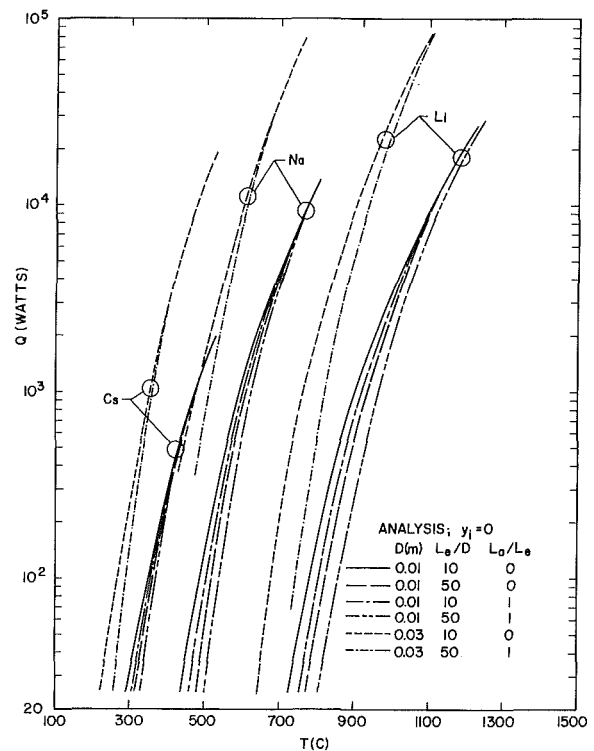


Fig. 6 The effect of vapor diameter, evaporator, and adiabatic lengths on the sonic heat flux limit for Li, Na, and Cs

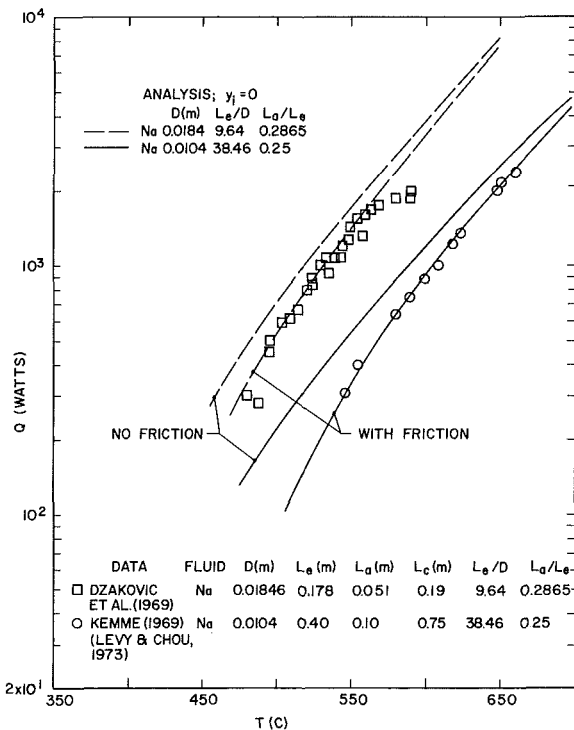


Fig. 5 Comparison of analytic results, with choking at the adiabatic section exit and with and without friction, with data

discussed earlier. At lower temperatures, the heat pipe performance becomes sensitive to the frictional effects, and the axial heat transfer capacity can be considerably reduced as illustrated in Fig. 5, which shows a good comparison of analysis with data with a finite length of the adiabatic region. The data in Fig. 5 are also predicted with the numerical model of Levy and Chou (1973) when they accounted for the frictional effects in evaporator and condenser.

The effects of the vapor diameter D , evaporator length to diameter ratio L_e/D , and adiabatic length to evaporator length ratio L_a/L_e , on the sonic heat transfer limits for lithium, sodium, and cesium are illustrated in Fig. 6. At constant D , an increase of the evaporator and adiabatic lengths has the effect of reducing the heat pipe's axial heat transport capacity; this reduction is considerable for long heat pipes and at lower temperatures where the frictional effects become more important. With the temperature and evaporator and adiabatic lengths fixed, a heat pipe with a larger vapor flow area can transport larger axial heat fluxes for all fluids in Fig. 6. The axial heat transport capacities of Li are also more sensitive to the frictional effects (and, therefore, on L_a and L_e) than those of Na, K, and Cs.

Figure 7 shows the effect of the non-normal-to-the-main-flow vapor injection in the evaporator ($y_i > 0$). Large values of y_i are seen to produce a considerable decrease of the sonic heat transfer limits for Li and Na at lower temperatures and a slight increase beyond the frictionless sonic heat transfer limit at very high temperatures. The physical explanation of these results is that at lower temperatures the frictional effects are important, whereas at higher temperatures the inertial effects dominate and require higher axial heat fluxes for $y_i > 0$ than for $y_i = 0$ for attainment of the sonic limit (see equation (24)). The non-normal-to-the-main-flow vapor injection has not been previously investigated and may be present in some systems where heat pipes are integrally built into the systems' structures.

Equation (24) also shows that an area increase for the vapor flow in the evaporation and adiabatic regions of a heat pipe can produce larger sonic heat transfer limits than in a uniform area pipe. This implies that heat pipes with long evaporator and adiabatic sections may require nonuniform cross-sectional areas for vapor flow ($dA/dx > 0$) in order to compensate for the reduction of sonic heat transfer limits brought about by the frictional effects. For applications to nuclear reactors in space, a super heat pipe system may be envisioned with a heat source supplying heat to variable cross-sectional areas of heat

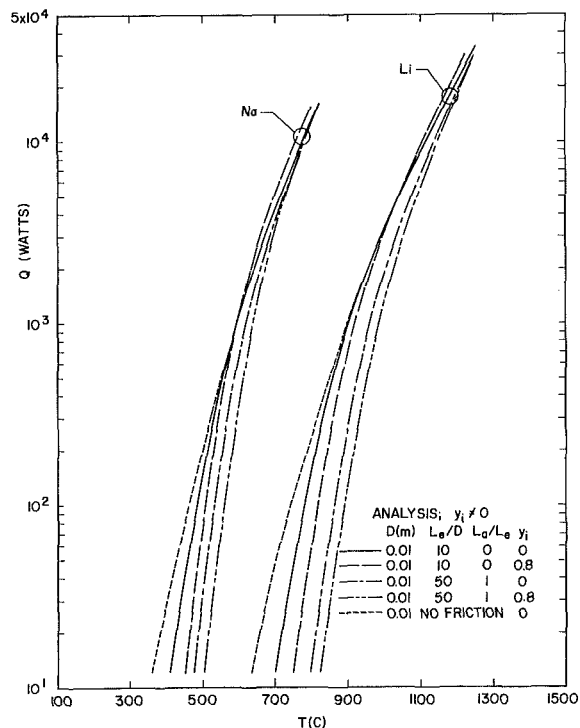


Fig. 7 The effect of variable y_i on the sonic heat flux limits for L_i and N_a

pipe evaporators that in turn transfer this heat to the power conversion system that may be removed by a considerable distance from the power source. In this manner a more compact reactor design can be achieved than by utilizing constant and large-diameter heat pipes.

4 Summary and Conclusions

The current designs of terrestrial and space-based systems use heat pipes for a variety of tasks. These applications require optimum heat pipe performance over a large range of system and environmental conditions. For these reasons, the heat pipe design has strived toward the development of super heat pipes that transfer optimum heat transfer rates without exceeding the heat transfer operating limits. Many of these limits may be suppressed and some may be eliminated through a judicious optimization of heat pipe geometry and selection of working fluids.

In the paper an analytical model has been presented for the design of high-temperature heat pipes with the sonic flow limiting the axial heat transport capacity. It was shown that

the sonic heat transfer limit is affected by the working fluid, vapor flow area, manner of vapor introduction into the vapor core region of the evaporator, and lengths of the evaporator and adiabatic regions. Achieving high rates of heat transfer requires large vapor flow cross-sectional areas, small lengths of the evaporator and adiabatic regions or a vapor flow area increase in these regions, and normal-to-the-main-flow liquid evaporation in the evaporator. A comparison of the analytical results with data of high-temperature heat pipes operating with sonic heat transfer limits is shown to be reasonable. The presented model can be readily adopted for the optimization of high-temperature heat pipe design.

References

- Bankston, C. A., and Smith, H. J., 1971, "Incompressible Laminar Vapor Flow in Cylindrical Heat Pipes," ASME Paper No. 71-WA/HT-15.
- Barthelemy, R. R., Massie, L. D., and Borger, W. U., 1986, "Military Space Power Systems Technology for the Twenty-First Century," *Intersociety Energy Conversion Engineering Conference*, Vol. 3, pp. 1401-1404.
- Busse, C. A., 1973, "Theory of the Ultimate Heat Transfer Limit of Cylindrical Heat Pipes," *Int. J. Heat Mass Transfer*, Vol. 16, pp. 169-186.
- Busse, C. A., 1986, Personal Communications.
- Desanctis, C., Priest, C., and Wood, W., 1986, "Space Station Overview," Paper No. AIAA-86-0315.
- Dobran, F., 1987a, "Heat Pipe Research and Development in the Americas," *Proc. 6th International Heat Pipe Conference*, May 25-28, Grenoble, France; also in *Heat Recovery Systems & CHP*, Vol. 9, 1989, pp. 67-100.
- Dobran, F., 1987b, "Super Heat Pipe Design Considerations for Applications to Space-Based Systems," *Int. Symp. on Thermal Problems in Space-Based Systems*, F. Dobran and M. Imber, eds., ASME, New York, pp. 1-12.
- Dzakowic, G., Tang, Y., and Arcella, F., 1969, "Experimental Study of Vapor Velocity Limit in a Sodium Heat Pipe," ASME Paper No. 69-HT-21.
- Kemme, J. E., 1966, "Heat Pipe Capability Experiments," *IEEE Thermionic Conversion Conference*, pp. 159-168.
- Kemme, J. E., 1969, "Ultimate Heat Pipe Performance," *IEEE Transactions on Electron Devices*, Vol. ED-16, pp. 717-723.
- Levy, E. K., 1968, "Theoretical Investigation of Heat Pipes Operating at Low Vapor Pressures," *ASME Journal of Engineering for Industry*, Vol. 90, pp. 547-522.
- Levy, E. K., and Chou, S. F., 1973, "The Sonic Limit in Sodium Heat Pipes," *ASME JOURNAL OF HEAT TRANSFER*, Vol. 95, pp. 218-223.
- Merrigan, M. A., Martinez, E. H., Keddy, E. S., Runyan, J. E., and Kemme, J. E., 1983, "Performance Demonstration of a High Power Space Reactor Heat Pipe Design," *Intersociety Energy Conversion Engineering Conference*, Vol. 4, pp. 1874-1879.
- Merrigan, M. A., Keddy, E. S., Sena, J. T., and Elder, M. G., 1984, "Heat Pipe Technology Development for High Temperature Space Radiator Applications," *Intersociety Energy Conversion Engineering Conference*, Vol. 1, pp. 592-597.
- Merrigan, M. A., 1986, "Heat Pipe Design for Space Power Heat Rejection Applications," *Intersociety Energy Conversion Engineering Conference*, Vol. 3, pp. 1993-1998.
- Quaile, J. P., and Levy, E. K., 1975, "Laminar Flow in a Porous Tube With Suction," *ASME JOURNAL OF HEAT TRANSFER*, Vol. 97, pp. 66-71.
- Sadunas, J. A., and Lehtinen, A., 1985, "Thermal Management Systems Options for the High Power Space Platforms," Paper No. AIAA-85-1047.
- Shapiro, A. H., 1953, *Compressible Fluid Flow*, Vol. 1, Ronald, New York.
- Vanlandingham, E. E., 1986, "The NASA Space Power Technology Program," *Intersociety Energy Conversion Engineering Conference*, Vol. 3, pp. 1405-1410.